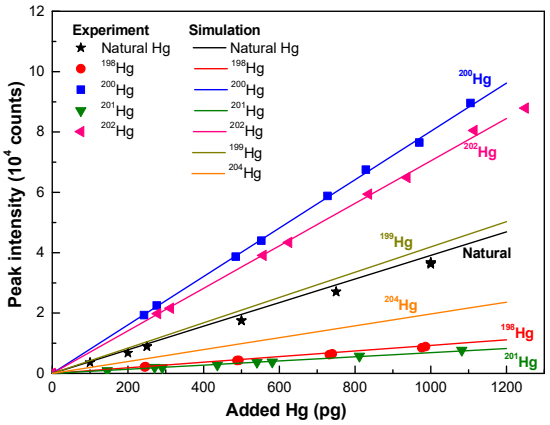
Experiment
Natural Hg
198Hg
200Hg
201Hg
202Hg
Simulation
Natural Hg
198Hg
200Hg
201Hg
202Hg
199Hg
204Hg
Peak intensity (10^4 counts)
Added Hg (pg)
0
2
4
6
8
10
12
0
200
400
600
800
1000
1200
200Hg
202Hg
199Hg
Natural
204Hg
198Hg
201Hg

The Application and Potential Artifacts of Zeeman Cold Vapor Atomic Absorption Spectrometry in Mercury Stable Isotope Analysis

Xia Lu,[1,2,#,*] Jiangtao Zhao,[3#] Xujun Liang,[2,#] Lijie Zhang,[2] Yurong Liu,[2] Xiangping Yin,[2] Xiangkai Li,[1] Baohua Gu[2,4,*]

[1]Key Laboratory of Cell Activities and Stress Adaptations, School of Life Sciences, Lanzhou University, Lanzhou 730000, China

[2]Environmental Sciences Division, Oak Ridge National Laboratory, Oak Ridge, TN 37831, USA

[3]School of Nuclear Science and Technology, Lanzhou University, Lanzhou 730000, China

[4]Department of Biosystems Engineering and Soil Science, University of Tennessee, Knoxville, TN 37996, USA

[#] These authors contributed equally.

ABSTRACT

Zeeman cold vapor atomic absorption spectrometry (CVAAS) has been widely used for environmental mercury (Hg) detection and quantification for decades, but little is known about its utility and potential artifacts in analyzing Hg with varying isotope compositions. We show that each Hg isotope responds differently by CVAAS analysis, with ^{200}Hg and ^{202}Hg isotopes exhibiting ~10 times greater signal intensities than ^{198}Hg and ^{201}Hg isotopes. However, all Hg isotopes show a linear correlation between Hg concentrations and the signal intensity, validated by both measurements and theoretical simulations. Zeeman CVAAS could thus offer a convenient, inexpensive tool for determining Hg isotopes, particularly in using single- or dual-labeled Hg isotopes for tracing Hg biogeochemical transformations, such as partitioning, ion exchange, sorption-desorption, and methylation-demethylation in environmental matrixes. We also caution that care must be taken when CVAAS is used for quantifying Hg in samples with changing isotope compositions to avoid measurement errors.

INTRODUCTION

Cold vapor atomic absorption spectrometry (CVAAS) is widely used for mercury (Hg) detection and quantification in environmental samples because of its high sensitivity, capable of detecting sub-picogram (pg) quantities of Hg.[1-5] It is also a preferred choice for field and air monitoring applications because of its affordability and portability.[1,2,6] However, a common issue with CVAAS is potential interferences resulting from molecular absorption of gaseous impurities, such as benzene. To resolve this issue, Zeeman background correction is used to improve the sensitivity, selectivity, and measurement accuracy.[7,8] This is done by splitting the Hg resonance line (λ=254 nm) into three polarized Zeeman components (π, σ^-, σ^+), although the photodetector detects only the radiation of two σ components (see Supporting Information (SI) "Zeeman CVAAS and theory" for details). The σ components are separated by the polarization modulator, and the spectral shift of the σ components is less than 0.1 nm or equivalent to a frequency of ~22 GHz (due to the hyperfine structure of Hg), which is much smaller than the widths of molecular absorption bands and/or scattering spectra of most interfering molecules. When the light passes through the sample chamber, the signal intensity is defined by the difference between the intensities of the two σ components of the sample.[7] Consequently, the background absorption from any interferences in σ^- and σ^+ is always the same and thus canceled. However, the absorption line profiles of most Hg isotopes fall within the σ^- component, except ^{199}Hg, which falls mostly in the σ^+ component (SI, Zeeman CVAAS and theory, Figure S1). The difference between σ^- and σ^+ intensities thus changes with changing Hg isotope compositions and their vapor concentrations, thereby providing a tool for quantifying Hg or Hg isotope concentrations.

Mercury has six stable isotopes with high natural abundances ranging from 6.9% to 29.9%. Enriched Hg isotopes are often used as tracers for investigating Hg fate and transformations in environmental systems, such as transport, sorption-desorption, methylation-demethylation, precipitation-dissolution, biological uptake, and ion exchange reactions.[9-13] However, to date few studies have taken the advantage of Zeeman CVAAS for quantifying Hg isotopes,[8] a technique that has been largely overlooked

in both laboratory and field investigations. Equally important is to realize that, if the Hg isotope effect is not considered, CVAAS analysis could potentially lead to large measurement errors if Hg isotope compositions in the reactant and the product change over the course of reactions. Although cold vapor atomic fluorescence spectrometry (CVAFS) is also widely used because of its low cost, it does not discriminate Hg isotopes as CVAFS measures the broad atomic fluorescence of Hg.[14,15]

The primary objective of this study was to demonstrate potential artifacts and the practical utility of Zeeman CVAAS for determining Hg isotopes in tracing Hg biogeochemical transformations, such as partitioning and concurrent Hg sorption-desorption reactions, in environmental matrixes. We provide theoretical basis for quantifying individual Hg isotopes or their mixtures and compare the advantages and disadvantages of using CVAAS for Hg isotope analyses. We suggest that CVAAS could offer a convenient, inexpensive tool for quantifying Hg isotopes without using specialized equipment, such as inductive coupled plasma–mass spectrometer (ICP-MS).[9,12,13]

MATERIALS AND METHODS

Standard solution of the natural Hg (1 μg mL^{-1} in 2% HNO_3) was purchased from Brooks Rand Laboratories (Seattle, WA). Enriched Hg stable isotopes (^{198}Hg, ^{200}Hg, ^{201}Hg, and ^{202}Hg) were supplied by Oak Ridge National Laboratory, Oak Ridge, Tennessee, and the purity of these isotopes is certified as follows: ^{198}Hg (92.78%), ^{200}Hg (96.41%), ^{201}Hg (96.17%), and ^{202}Hg (95.86%).[11] All impurity isotopes are listed in Supporting Information (SI Table S1). These isotopes were received as HgO or $HgCl_2$ solids, and their stock solutions were prepared by dissolving HgO or $HgCl_2$ in 1–3% HCl and diluting to 1 mg/L in 1% HCl. The concentration of each Hg isotope was validated by ICP-MS analysis (Elan DRC-e, PerkinElmer Inc.). The isotope and natural Hg working solutions at 10 μg/L were preserved in 0.5% BrCl, and an aliquot (in the mass range of 200–1200 pg) was used and analyzed by CVAAS (Lumex RA-915+, Ohio Lumex Co.), as described previously.[3-5,16,17] The peak intensity as a function of the Hg mass or concentration was plotted by linear fitting using the OriginPro software (OriginLab).[5]

Standard additions of Hg isotopes were performed to evaluate the utility and artifacts by CVAAS analyses in an environmental water sample obtained from the contaminated East Fork Poplar Creek (EFPC) in Oak Ridge, Tennessee, as described previously.[18, 19] The filtered water contained ~3 mg/L dissolved organic matter and 25 ng/L Hg at pH 7.8. Following the addition of a Hg isotope (~85 ng/L), the total Hg (THg) concentration was determined after samples were oxidized in BrCl (5% v/v) overnight.[3,4,20,21] Additionally, sequential extraction was used to compare the partitioning and immobilization of the freshly added ^{200}Hg (as a tracer) with previously deposited old Hg in a contaminated EFPC soil.[22,23] The extractable pools of Hg included (1) deionized water, (2) 0.01M HCl/0.1M acetic acid, (3) 1M KOH, (4) 12M nitric acid, and (5) aqua regia, and were used as a proxy of Hg bioavailability in soil (see SI "Hg sequential extraction").[22,23] Furthermore, concurrent Hg adsorption and desorption on mineral hematite were conducted using dual-labeled Hg isotopes (e.g., ^{200}Hg and ^{198}Hg), in which ^{200}Hg (17 μg/L) was equilibrated with hematite first for 24 h, followed by the addition of a small aliquot (40 μL) of ^{198}Hg (15 μg/L, final concentration). Hematite particles were then removed by filtration (0.2 μm), and Hg concentrations in supernatant solutions before and after ^{198}Hg addition were determined. The amounts of ^{198}Hg and ^{200}Hg adsorbed (or ^{200}Hg desorbed) were calculated by the difference between the amounts added and that found in the supernatant solution. The average concentrations of duplicate samples were reported, and error bars represent the deviation between the two replicates (X1 and X2), defined as the absolute value of (X1–X2)/2.

The CVAAS method detection limit (MDL) was determined for four available Hg isotopes (^{198}Hg, ^{200}Hg, ^{201}Hg, and ^{202}Hg) in both deionized water and the simulated water consisting of 1 mM $NaHCO_3$, 2 mM $CaCl_2$, 2 mM $MgCl_2$, and 1 mM $ZnCl_2$ as interfering ions.[24] No significant differences were observed between samples prepared in deionized water or the simulated water (SI Figure S2) since all Hg was converted to gaseous elemental Hg(0) by Sn(II) reduction and ultimately detected by CVAAS. Therefore, MDLs were computed as an average (from deionized water and the simulated water). They were 8.08±1.78, 3.90±0.73, 13.54±1.96, and 3.13±0.12 pg for ^{198}Hg, ^{200}Hg, ^{201}Hg, and ^{202}Hg, respectively.

RESULTS AND DISCUSSION

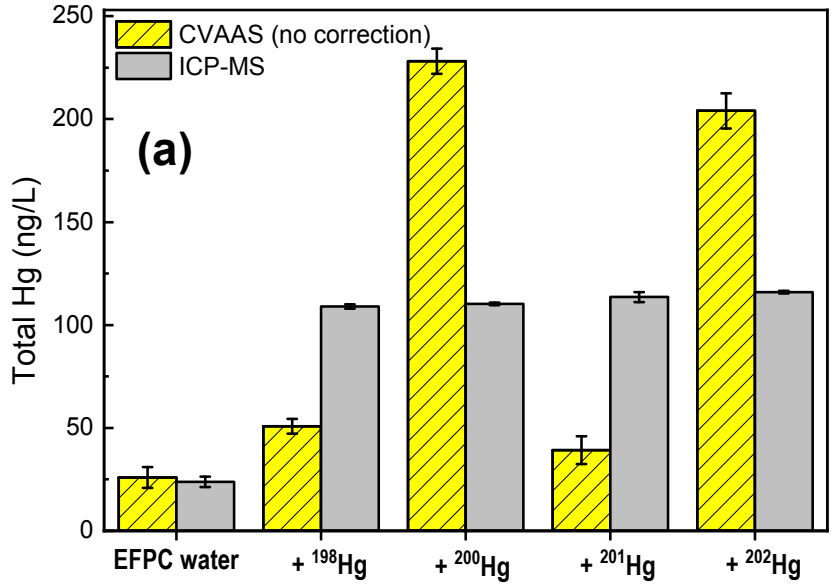

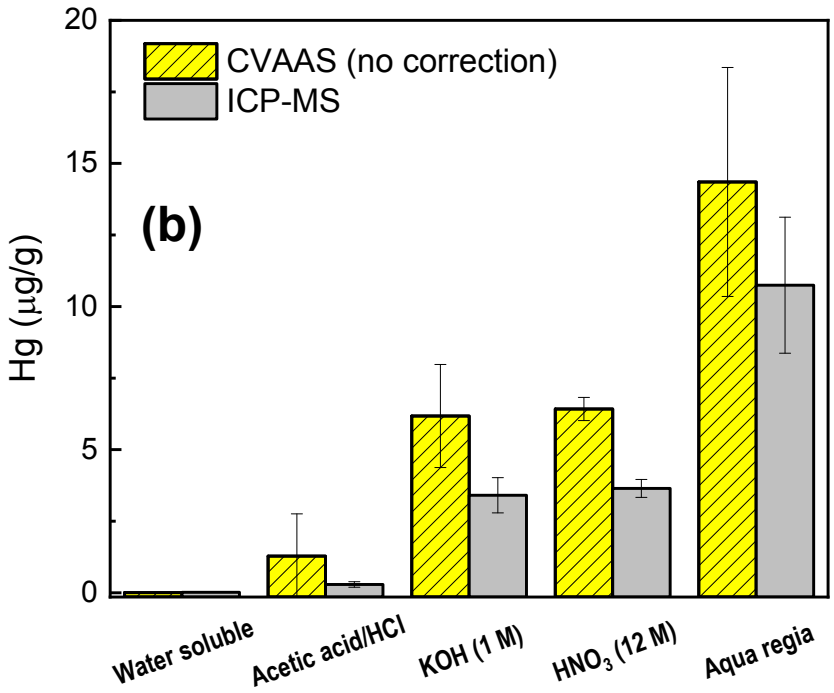

Figure 1. Comparisons between Zeeman CVAAS and ICP-MS for determining Hg concentrations in environmental matrixes. (a) EFPC creek water spiked with or without Hg stable isotopes of ^{198}Hg, ^{200}Hg, ^{201}Hg, and ^{202}Hg (85 ng/L each), and (b) sequential extraction of Hg in a contaminated EFPC soil with freshly added ^{200}Hg as a tracer (see SI, Hg sequential extraction for details).[22, 23] Without correction of the Hg isotope effect, CVAAS analysis results in large measurement errors.

"Artifacts" by Zeeman CVAAS analysis

Potential artifacts associated with Zeeman CVAAS analyses of Hg isotopes in environmental matrixes were first realized during measurements of Hg concentrations in the contaminated EFPC water by standard addition of Hg isotopes of ^{198}Hg, ^{200}Hg, ^{201}Hg, or ^{202}Hg (85 ng/L each). Using standard calibration of the ambient natural Hg, we found that the measured THg concentrations after additions of ^{201}Hg, ^{198}Hg, ^{202}Hg, and ^{200}Hg were 39.2, 50.8, 204.1, and 228.2 ng/L, respectively (Figure 1a), whereas the anticipated THg should be ~110 ng/L (analyzed by ICP-MS) (as the creek water contained ~25 ng/L Hg). The results thus indicate that, for samples spiked with ^{198}Hg and ^{201}Hg, CVAAS substantially underestimated the Hg concentration by 64.4% and 53.8%, respectively, but overestimated the Hg concentration by 85.5% and 107.5% in samples spiked with ^{202}Hg, and ^{200}Hg, respectively.

Similarly, in a comparative study of sequential extraction of the previously deposited Hg and the freshly added ^{200}Hg (as a tracer) in a contaminated EFPC soil (SI, Hg sequential extraction),[22] we found that CVAAS substantially overestimated the four extractable fractions of Hg when compared to the amounts analyzed by ICP-MS (Figure 1b). The measured THg concentrations by CVAAS in fractions of water, acetic acid/HCl, KOH, HNO_3, and aqua regia were 0.01, 1.28, 6.17, 6.42 and 14.35 μg/g, respectively, compared to the ICP-MS measured concentrations of 0.01, 0.29, 3.41, 3.46, and 10.75 μg/g, respectively (Figure 1b). In total, CVAAS overestimated the extractable Hg by about 56%. The result again signifies serious measurement artifacts by CVAAS when the Hg isotope is used as a tracer and the isotope effect is not accounted for (described below).

Theory and utility of Zeeman CVAAS in Hg isotope analysis

To provide theoretical basis for the observed CVAAS measurement errors (Figure 1), we analyzed four Hg isotopes in hand, including ^{198}Hg, ^{200}Hg, ^{201}Hg, and ^{202}Hg, and performed simulations of CVAAS responses to all six Hg isotopes (SI, Zeeman CVAAS and Theory). Results indicate that each Hg isotope gave vastly different signal responses by CVAAS (Figure 2a). With the same amount of Hg added to solution (200–1200 pg), the measured peak intensities of ^{200}Hg and ^{202}Hg were ~10 times higher than

142 those of ^{201}Hg and ^{198}Hg, although they all showed a linear correlation with the added Hg mass. The
143 measured slopes of the signal intensity against the added Hg mass were 83.41±0.36, 73.65±0.40,
144 9.46±0.07, and 7.21±0.10 counts/pg for ^{200}Hg, ^{202}Hg, ^{198}Hg, and ^{201}Hg, respectively. Obviously, these
145 large differences in CVAAS responses to Hg isotopes explained large discrepancies observed when Hg
146 isotope tracers were used in the standard addition and sequential extraction experiments (Figure 1), in
147 which Hg isotope effects were not accounted for. However, when corrected using the calibration curve (or
148 the slope) of each Hg isotope shown in Figure 2a, the measured Hg concentrations by CVAAS matched
149 well with those determined by ICP-MS (SI Figure S3).

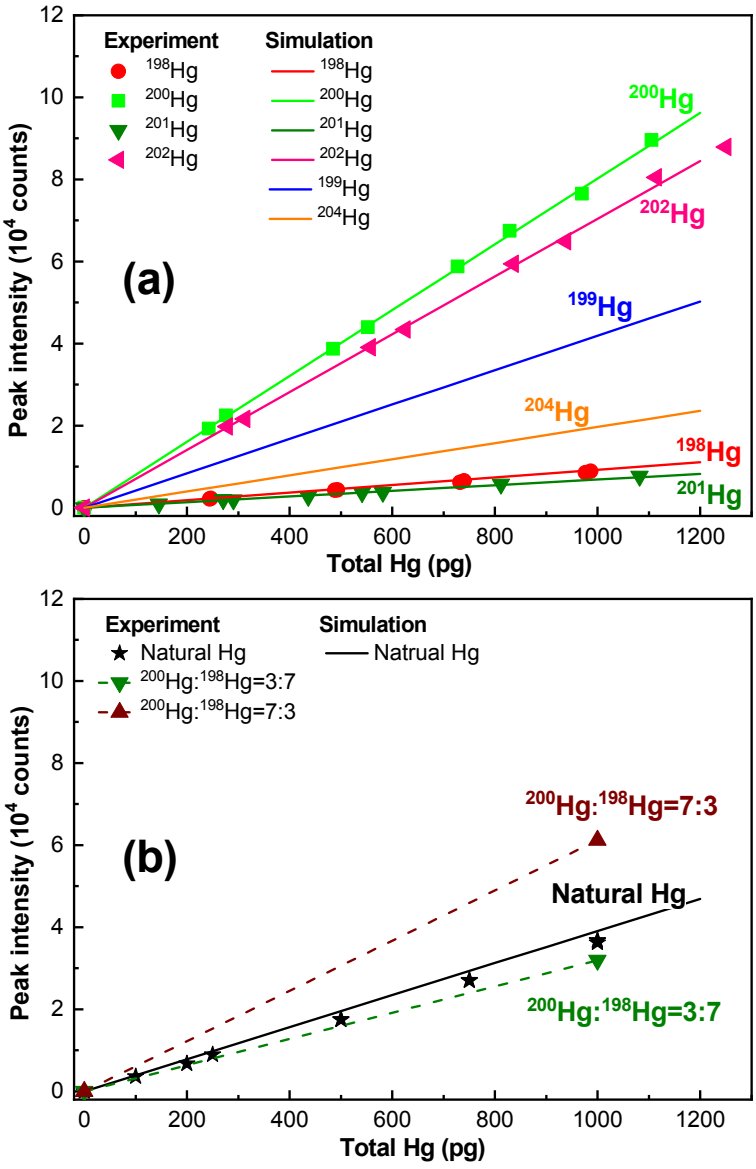

150

Figure 2. Zeeman CVAAS determination of (a) ^{198}Hg, ^{200}Hg, ^{201}Hg, and ^{202}Hg isotopes (symbols) and the simulation results (solid lines), and (b) mixed isotopes of ^{200}Hg and ^{198}Hg, and the natural Hg.

Why Hg isotopes respond differently by CVAAS is attributed to the absorption profiles of the hyperfine structures of Hg which overlap with Zeeman σ^- and σ^+ components of the light source profile (SI, Zeeman CVAAS and Theory; Figure S1). As described earlier, the absorption line profiles of most Hg isotopes fall within the σ^- component, except ^{199}Hg and part of ^{201}Hg, which fall within the σ^+ component. The difference between signal intensities of σ^- and σ^+ components changes with changing Hg isotope compositions and concentrations and is defined by Eq. 1 (SI, Zeeman CVAAS and Theory). Using Eq. 1, we can simulate the signal response to each individual Hg isotope, and the simulation results for ^{198}Hg, ^{199}Hg, ^{200}Hg, ^{201}Hg, ^{202}Hg, and ^{204}Hg were plotted in Figure 2a as solid lines. The calculated slopes are also listed in SI Table S2, in which Columns 4 and 5 are the adjusted slopes, corrected for impurities present in the four measured Hg isotopes. The simulation results showed an excellent agreement with the measured values (symbols) of four Hg isotopes (^{198}Hg, ^{200}Hg, ^{201}Hg, ^{202}Hg). Data for ^{199}Hg and ^{204}Hg were not available because of their limited source availability. However, for all Hg isotopes, simulation results gave a linear relationship between the signal intensity and the Hg concentration (Figure 2a), although the slope varied with different Hg isotopes due to their differences in hyperfine structures.

Both experiments and simulations (Figure 2a) clearly show the usefulness of CVAAS for quantitative analyses of Hg isotopes because each Hg isotope gives a linear correlation and a distinct slope, which is a constant for a given instrument with preset conditions. Importantly, when the two Hg isotopes were mixed in solution, we found that the measured slope was additive, equal to the sum of the products of the slope and the mass fraction of each isotope in the mixture. For example, at the ^{200}Hg to ^{198}Hg atomic ratio of 3:7, the slope of the total Hg (THg = ^{200}Hg + ^{198}Hg) was calculated to be 31.65 (=0.3×83.41 + 0.7×9.46), which is in excellent agreement with the measured slope of 31.92 (Figure 2b, dashed line and symbol). Similarly, at the ^{200}Hg to ^{198}Hg ratio of 7:3, the measured slope of the mixture

was 61.23, consistent with the calculated slope of 61.23 (Figure 2b). We also measured the instrument response to the natural Hg and observed a slope of 36.24±0.17 (Figure 2b). However, this slope was lower than the expected additive value of the four measured Hg isotopes (SI Table S2) and their respective natural abundances (i.e., ^{198}Hg, 9.97%; ^{200}Hg, 23.10%; ^{201}Hg, 13.18%; ^{202}Hg, 29.86%). The expected slope of the natural Hg should be at least 41.45 (by accounting the four measured isotopes), if all Hg isotopes would obey the additive rule described above. The main cause of this deviation is attributed to the ^{199}Hg hyperfine structure overlapping mostly with the σ^+ component, and its signal intensity is therefore subtractive when mixed with other Hg isotopes (SI, Eq. 1). This result thus explained why the measured slope of the natural Hg was lower than the value expected from the summation of the four measured isotopes (^{198}Hg, ^{200}Hg, ^{201}Hg, ^{202}Hg). Therefore, except for ^{199}Hg, the signal intensity of any of the mixed isotopes of ^{198}Hg, ^{200}Hg, ^{201}Hg, ^{202}Hg, and ^{204}Hg equals to the summation of each individual Hg isotope, confirmed by the measured values of any binary mixtures of ^{198}Hg and ^{200}Hg at varying atomic ratios (Figure 2b; SI Figure S4a) or a mixed sample containing ^{198}Hg, ^{200}Hg, ^{201}Hg, and ^{202}Hg (SI Figure S4b). These results thus indicate the robustness of using CVAAS as a tool for Hg isotope analysis.

Environmental applications of CVAAS for Hg isotope tracer studies: Pros and Cons

Enriched Hg isotopes are often used in tracing Hg biogeochemical transformations in both laboratory and field investigations,[9-13] such as standard addition, sorption and desorption, methylation and demethylation, and ion exchange reactions in environmental systems. As illustrated in Figure 1b, sequential extraction was used to assess Hg species distributions between the freshly added ^{200}Hg tracer (after 24 h) and the old Hg in a contaminated EFPC soil.[22, 23] The freshly added ^{200}Hg was determined after subtracting the old Hg in the untreated soil (without ^{200}Hg). Based on the measured ^{200}Hg calibration curve (Figure 2a, Table S2), we found that the distribution of ^{200}Hg in extractable pools resembled the old Hg (Figure 3a), in which negligible amounts of ^{200}Hg were found in water- and acetic acid/HCl-extractable pools (presumably more bioavailable than other Hg pools). Most of the added ^{200}Hg seems immobilized in the pools associated with soil organic matter (1M KOH) and minerals (12M HNO_3 and aqua regia) (Figure 3a). These results confirm previous observations that freshly added Hg is often rapidly

immobilized and becomes unavailable for biological uptake,[10, 25] although detailed discussion of the mechanisms of Hg immobilization in soil is beyond the scope of this work.

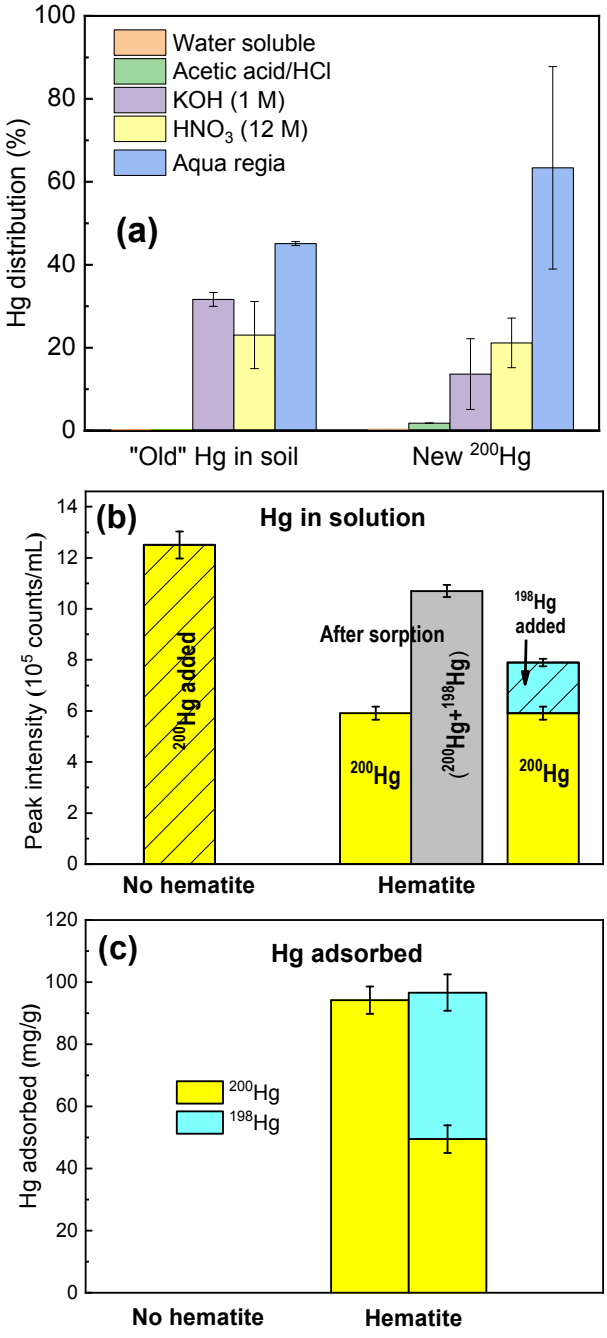

Figure 3. (a) Comparisons between the new, freshly added ^{200}Hg (as a tracer) and old Hg species distributions in a contaminated EFPC soil by sequential extraction.[22, 23] (b, c) Determination of ^{200}Hg sorption and then desorption by ^{198}Hg on hematite (0.1 g/L) at pH 6.5. The initially added ^{200}Hg was 17 µg/L. After equilibration with hematite, approximately an equal molar concentration of ^{198}Hg (~15 µg/L) was added. Plot (b) is the measured CVAAS peak intensities of ^{200}Hg and (^{200}Hg +^{198}Hg) in solution before and after their adsorption on hematite, and (c) is the amount of Hg adsorbed on hematite.

Perhaps the most important application of CVAAS is the use of dual-labeled Hg isotopes (e.g., ^{200}Hg and ^{198}Hg) to trace simultaneous Hg transformations in environmental systems, such as concurrent Hg adsorption and desorption reactions, as illustrated in Figure 3b,c. Because of a large difference (~10×) in CVAAS responses to ^{200}Hg and ^{198}Hg (Figure 2a, Table S2), any desorption or displacement of one Hg isotope by the other could be readily detected. Results show that, after pre-equilibration of ^{200}Hg with hematite for 24 h, the CVAAS intensity in the supernatant decreased from 12.51×10^5 (Initial) to 5.67×10^5 counts/mL (Figure 3b, 2nd column). However, a substantially increased intensity (10.3×10^5 counts/mL) was observed (Figure 3b, 3rd column) following the addition of ^{198}Hg. This intensity was much higher than that expected (7.6×10^5 counts/mL, Figure 3b, 4th column) by the summation of ^{200}Hg (assuming no desorption) and the total added ^{198}Hg in solution (assuming no adsorption of ^{198}Hg). Evidently, a large fraction of the pre-adsorbed ^{200}Hg was desorbed by ^{198}Hg, resulting in a substantially increased intensity because CVAAS response of ^{200}Hg is ~10 times higher than that of ^{198}Hg (SI Table S2). Since the supernatant solution now contained both ^{200}Hg and ^{198}Hg, the measured total intensity cannot be directly converted to the Hg concentration unless the THg concentration or the ratio of ^{200}Hg to ^{198}Hg in solution is known. In this case, THg is quantified using techniques such as CVAFS, as described earlier, so that ^{200}Hg and ^{198}Hg in solution can be calculated using the slopes given in Table S2, and the amounts of ^{200}Hg and ^{198}Hg adsorbed on hematite determined (Figure 3c). Interestingly, we found that the addition of ^{198}Hg to the hematite suspension that had been pre-equilibrated with ^{200}Hg resulted in desorption or exchange of ^{200}Hg by ^{198}Hg and led to approximately an equal distribution of ^{200}Hg and ^{198}Hg on hematite.

Together, these two case studies (Figure 3) demonstrate the practical utility of Zeeman CVAAS for accurate determination of single or dual-labeled Hg isotopes in studies such as tracing Hg fate and transport, sorption-desorption, and transformation reactions in environmental systems, as reported previously.[9-13] Another major advantage of using Zeeman CVAAS is its low detection limit, field portability, and wide availability in many Hg labs because of its low cost (~10× less expensive than a typical ICP-MS). It could also be used in real-time analysis and monitoring. A disadvantage is that CVAAS measures the total signal intensity and cannot resolve individual Hg isotopes when mixed.

Fortunately, most tracer studies use only one or two Hg isotopes (Figure 3). In the latter case, only a secondary measurement is necessary to determine the THg by techniques such as CVAFS and ICP-MS. However, regardless of its application, realizing the utility and potential artifacts of CVAAS in Hg isotope analysis is critically important, as it is among the most widely used technique for Hg quantification and monitoring in both laboratory and field investigations.

ASSOCIATED CONTENT

Supporting Information

All data needed to evaluate the conclusions in the paper are present in the paper and/or the Supporting Information, which is available free of charge via the Internet at http://pubs.acs.org.

AUTHOR INFORMATION

Corresponding author:

Email: gub1@ornl.gov; lux@lzu.edu.cn

Notes:

The authors declare no competing financial interest.

ACKNOWLEDGMENTS

This research was sponsored by the Office of Biological and Environmental Research within the Office of Science of the U.S. Department of Energy (DOE), as part of the Mercury Science Focus Area project at the Oak Ridge National Laboratory (ORNL) and by the National Natural Science Foundation of China (41807477). The Department of Energy will provide public access to these results of federally sponsored research in accordance with the DOE Public Access Plan (http://energy.gov/downloads/doe-public-access-plan). ORNL is managed by UT-Battelle, LLC under Contract No. DE-AC05-00OR22725 with DOE.

REFERENCES

1. Hadeishi, T., Isotope-shift Zeeman effect for trace-element detection - Application of atomic physics to environmental problems. *Appl. Phys. Lett.* **1972,** *21* (9), 438-440.

2. Brooks, S. C.; Southworth, G. R., History of mercury use and environmental contamination at the Oak Ridge Y-12 Plant. *Environ. Pollut.* **2011,** *159* (1), 219-228.

3. Gu, B.; Bian, Y.; Miller, C. L.; Dong, W.; Jiang, X.; Liang, L., Mercury reduction and complexation by natural organic matter in anoxic environments. *Proc. Natl. Acad. Sci. USA* **2011,** *108* (4), 1479-1483.

4. Lu, X.; Gu, W. Y.; Zhao, L.; Ul Haque, M. F.; DiSpirito, A. A.; Semrau, J. D.; Gu, B., Methylmercury uptake and degradation by methanotrophs. *Science Adv.* **2017,** *3*, e1700041.

5. Lu, X.; Johs, A.; Zhao, L.; Wang, L.; Pierce, E. M.; Gu, B., Nanomolar copper enhances mercury methylation by *Desulfovibrio desulfuricans* ND132. *Environ. Sci. Technol. Lett.* **2018,** *5* (6), 372-376.

6. Panichev, N. A.; Panicheva, S. E., Determination of total mercury in fish and sea products by direct thermal decomposition atomic absorption spectrometry. *Food Chem.* **2015,** *166*, 432-441.

7. Sholupov, S. E.; Ganeyev, A. A., Zeeman atomic-absorption spectrometry using high-frequency modulated light polarization. *Spectrochim Acta B* **1995,** *50* (10), 1227-1236.

8. Ganeyev, A. A.; Sholupov, S. E., New Zeeman atomic-absorption spectroscopy approach for mercury isotope analysis. *Spectrochim Acta B* **1992,** *47* (11), 1325-1338.

9. Jiang, P.; Li, Y. B.; Liu, G. L.; Yang, G. D.; Lagos, L.; Yin, Y. G.; Gu, B. H.; Jiang, G. B.; Cai, Y., Evaluating the role of re-adsorption of dissolved Hg2+ during cinnabar dissolution using isotope tracer technique. *J. Haz. Mater.* **2016,** *317*, 466-475.

10. Harris, R. C.; Rudd, J. W. M.; Amyot, M.; Babiarz, C. L.; Beaty, K. G.; Blanchfield, P. J.; Bodaly, R. A.; Branfireun, B. A.; Gilmour, C. C.; Graydon, J. A.; Heyes, A.; Hintelmann, H.; Hurley, J. P.; Kelly, C. A.; Krabbenhoft, D. P.; Lindberg, S. E.; Mason, R. P.; Paterson, M. J.; Podemski, C. L.; Robinson, A.; Sandilands, K. A.; Southworth, G. R.; Louis, V. L. S.; Tate, M. T., Whole-ecosystem study shows rapid fish-mercury response to changes in mercury deposition. *Proc. Natl. Acad. Sci. USA* **2007,** *104* (42), 16586-16591.

11. Olsen, T. A.; Brandt, C. C.; Brooks, S. C., Periphyton biofilms influence net methylmercury production in an industrially contaminated system. *Environ. Sci. Technol.* **2016,** *50* (20), 10843-10850.

12. Jonsson, S.; Skyllberg, U.; Nilsson, M. B.; Lundberg, E.; Andersson, A.; Bjorn, E., Differentiated availability of geochemical mercury pools controls methylmercury levels in estuarine sediment and biota. *Nature Comm.* **2014,** *5*, 4624.

13. Jonsson, S.; Skyllberg, U.; Nilsson, M. B.; Westlund, P. O.; Shchukarev, A.; Lundberg, E.; Bjorn, E., Mercury methylation rates for geochemically relevant hg-II species in sediments. *Environ. Sci. Technol.* **2012,** *46* (21), 11653-11659.

14. Bloom, N.; Fitzgerald, W. F., Determination of volatile mercury species at the picogram level by low-temperature gas-chromatography with cold-vapor atomic fluorescence detection. *Anal Chim Acta* **1988,** *208* (1-2), 151-161.

15. Bramanti, E.; D'Ulivo, A.; Lampugnani, L.; Zamboni, R.; Raspi, G., Application of mercury cold vapor atomic fluorescence spectrometry to the characterization of mercury-accessible -SH groups in native proteins. *Anal Biochem* **1999,** *274* (2), 163-173.

16. Liu, Y.; Lu, X.; Zhao, L.; An, J.; He, J. Z.; Pierce, E. M.; Johs, A.; Gu, B., Effects of cellular sorption on mercury bioavailability and methylmercury production by *Desulfovibrio desulfuricans* ND132. *Environ. Sci. Technol.* **2016,** *50*, 13335-13341.

17. Zhao, L.; Chen, H.; Lu, X.; Lin, H.; Christensen, G. A.; Pierce, E. M.; GU, B., Contrasting effects of dissolved organic matter on mercury methylation by *G. sulfurreducens* PCA and *D. desulfuricans* ND132. *Environ. Sci. Technol.* **2017,** *51*, 10468–10475.

18. Dong, W.; Liang, L.; Brooks, S. C.; Southworth, G.; Gu, B., Roles of dissolved organic matter in the speciation of mercury and methylmercury in a contaminated ecosystem in Oak Ridge, Tennessee. *Environ. Chem.* **2010,** *7* (1), 94–102.

19. Miller, C.; Southworth, G.; Brooks, S. C.; Liang, L.; Gu, B., Kinetic controls on the complexation between mercury and dissolved organic matter in a contaminated environment. *Environ. Sci. Technol.* **2009,** *43*, 8548-8553.

20. Hu, H.; Lin, H.; Zheng, W.; Tomanicek, S. J.; Johs, A.; Feng, X.; Elias, D. A.; Liang, L.; Gu, B., Oxidation and methylation of dissolved elemental mercury by anaerobic bacteria. *Nature Geosci.* **2013,** *6* (9), 751-754.

21. Lin, H.; Morrell-Falvey, J. L.; Rao, B.; Liang, L.; Gu, B., Coupled mercury-cell sorption, reduction, and oxidation affecting methylmercury production by *Geobacter sulfurreducens* PCA. *Environ. Sci. Technol.* **2014,** *48* (20), 11969-11976.

22. Miller, C. L.; Watson, D. B.; Lester, B. P.; Lowe, K. A.; Pierce, E. M.; Liang, L. Y., Characterization of soils from an industrial complex contaminated with elemental mercury. *Environ. Res.* **2013,** *125*, 20-29.

23. Bloom, N. S.; Preus, E.; Katon, J.; Hiltner, M., Selective extractions to assess the biogeochemically relevant fractionation of inorganic mercury in sediments and soils. *Analytica Chimica Acta* **2003,** *479* (2), 233-248.

24. Dong, W.; Liang, L.; Brooks, S.; Southworth, G.; Gu, B., Roles of dissolved organic matter in the speciation of mercury and methylmercury in a contaminated ecosystem in Oak Ridge, Tennessee. *Environ. Chem.* **2010,** *7* (1), 94-102.

25. Hintelmann, H.; Harris, R.; Heyes, A.; Hurley, J. P.; Kelly, C. A.; Krabbenhoft, D. P.; Lindberg, S.; Rudd, J. W. M.; Scott, K. J.; St Louis, V. L., Reactivity and mobility of new and old mercury deposition in a Boreal forest ecosystem during the first year of the METAALICUS study. *Environ. Sci. Technol.* **2002,** *36* (23), 5034-5040.